

COMMISSIONING AND OPERATION OF THE SPIRAL2 SC LINAC

A.K. Orduz*, P-E. Bernaudin, M. Di Giacomo, C. Jamet,
J-M. Lagniel, G. Normand and A. Savalle

Grand Accélérateur National d'Ions Lourds (GANIL), Caen, France
D. Uriot, IRFU, CEA, Université Paris-Saclay, Gif-sur-Yvette, France

Abstract

The SPIRAL2 linac is now successfully commissioned; H^+ , $^4He^{2+}$ and D^+ have been accelerated up to nominal parameters and $^{18}O^{6+,7+}$ and $^{40}Ar^{14+}$ beams have been also accelerated up to 7 MeV/A. The main steps with 5 mA H^+ , D^+ beams and with 0.8 mA $^{18}O^{6+}$ are described. The general results of the commissioning of the RF, cryogenic and diagnostics systems, as well as the preliminary results of the first experiments on NFS are presented. In addition of an improvement of the matching to the linac, the tuning procedures of the 3 Medium Energy Beam Transport (MEBT) rebunchers and 26 linac SC cavities were progressively improved to reach the nominal parameters in operation, starting from the classical “signature matching method”. The different cavity tuning methods developed to take into account our particular situation (very low energy and large phase extension) are described. The tools developed for an efficient linac tuning in operation, e.g. beam energy and intensity changes, choice of the optics to obtain the requested beam parameters on target... are also discussed.

INTRODUCTION

The Grand Accélérateur National d'Ions (GANIL) accelerator complex in France has now two machines in operation, the cyclotrons and the SC linear accelerator SPIRAL2 [1]. Research with these beams covers mainly nuclear physics, nuclear astrophysics and astrochemistry, as well as interdisciplinary topics such as materials irradiation, nanostructuring and radiobiology. These beams are also used to irradiate electronic components and polymer membranes [2]. In contrast to the original GANIL facility comprising 5 cyclotrons in operation since 1983, the SPIRAL2 linear accelerator started delivering beams in 2021 [3].

This new accelerator has two injectors (Low Energy Beam Transport LEBT1 and LEBT2), one for heavy ions with a mass-to-charge ratio $A/Q \leq 3$ and another for H^+ / D^+ beams, with maximum intensities of 1 mA and 5 mA CW, respectively. This is followed by the LBETc where the beam can be chopped with a frequency between 1 Hz to 100 kHz, and the intensity and emittance controlled by a set of 6 H and V slits [4, 5]. The MEBT includes three rebunchers for longitudinal beam tuning and one Single-Bunch-Selector (SBS) used for NFS experiments [6]. The SC linac is divided into a low β (0.07) and high β (0.12) section, the first one composed by 12 cryomodules, each containing 1 quarter wave resonator (QWR) designed by CEA and the second one composed by 7 cryomodules, each containing 2 QWR

designed by CNRS [7, 8]. A global layout of SPIRAL2 is shown in Fig. 1. Finally, three High Energy Beam Transport (HEBT) lines drive the beam to the experimental rooms Neutron For Science (NFS) and Super Separator Spectrometer (S^3), or to the main beam dump (SAFARI) [9, 10]. The diagnostics along the linac are located in the “warm sections” between cryomodules, as shown in Fig. 1, which contain the quadrupole doublets, Beam Position Monitors (BPMs), Beam Extension Monitors (BEMs) and vacuum gauges and pumping systems [11].

Table 1 summarizes the variety of beams available in SPIRAL2. The 4th column includes the parameters of the new injector NEWGAIN which is in the design phase and is described later in this paper.

Table 1: SPIRAL2 Beam Specifications

Parameter	H^+	D^+	$A/Q \leq 3$	$A/Q \leq 7$
A/Q	1	2	3	7
Max I (mA)	5	5	1	1
Max E (MeV/A)	33	20	14.5	7
Beam power (kW)	165	200	45	16

The linac commissioning was carried out between 2019 and 2021 at the same time as the transition to operation with first tests performed in NFS [12, 13]. H^+ , D^+ and $^4He^{2+}$ beams were successfully tuned and sent through the LEBT, Radio frequency Quadrupole (RFQ), MEBT, SC linac and HEBT to SAFARI at their nominal energy of 33 MeV for H^+ and 40 MeV for D^+ and $^4He^{2+}$ with 100% transmission. Results obtained during power ramps up to 16 kW with a H^+ beam and to 10 kW with a D^+ beam showed that SPIRAL2 can operate at its full power of 165 and 200 kW, respectively [1, 14]. Losses were studied and controlled by monitoring the 27 Beam Loss Monitors (BLMs) located along the linac and HEBT as shown in Fig. 1. In addition, the beam losses were controlled by different measurements such as the transmission with ACCT and DCCT, the vacuum pressure variation with vacuum gauges, the beam position and ellipticity with BPM and the segmented ring current with the temperature of SAFARI thermocouples [15].

Since 2022, SPIRAL2 delivers beams for physics experiments, mainly to the NFS room and also to carry out the preliminary studies for the S^3 commissioning in 2024. The studies carried out during 2022 were related to the heavy ions tuning and transport at low energy through the linac. This article focuses on the last commissioning results and the first year of operation of SPIRAL2. The first part presents the tuning process and the results of the first heavy ion ac-

* angie.orduz@ganil.fr

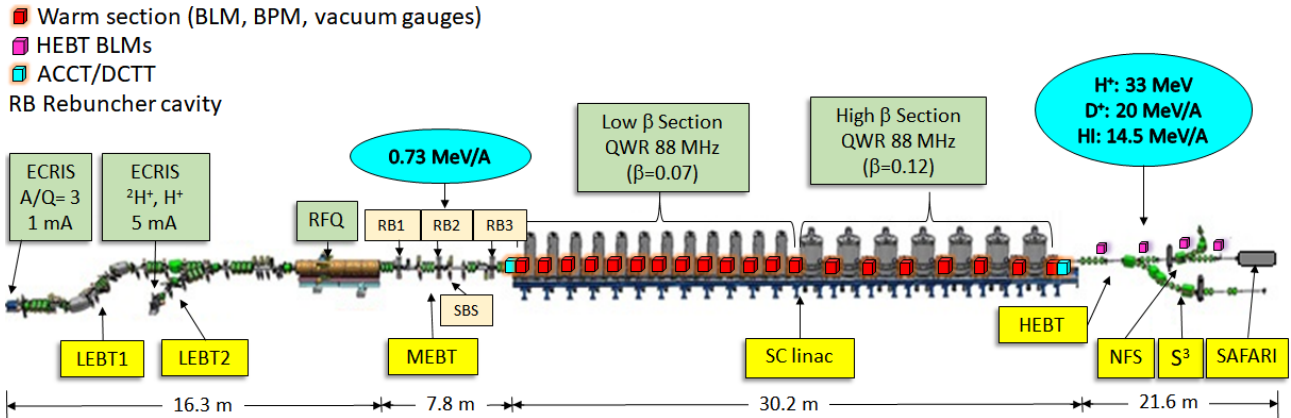


Figure 1: SPIRAL2 SC linac layout.

celeration. Finally, the second part describes the operation timetable in 2022, the development of applications to optimize the tuning procedures and the latest cryogenic and diagnostics systems improvements.

SPIRAL2 COMMISSIONING

The SPIRAL2 commissioning was successfully completed in 2021 with H^+ , D^+ and $^4He^{2+}$ beams. However, as part of the preparation for S^3 commissioning, heavy ion beams $^{18}O^{6+,7+}$ and $^{40}Ar^{14+}$ were tuned and accelerated in 2022. In order to access very low cross section in fusion reactions, S^3 demands low energy and high intensity beams, hence beam tunings were set for a maximum energy of 7 MeV/A [10].

The linac beam tuning was improved by a fine adjustment of the last two quadrupole fields and rebuncher #3 phase and voltage in the MEBT, reducing the losses. Also, the tuning strategy for operation has been improved since the commissioning and is now based on three methods. The first one, the "advanced method", is an evolution of the classical "signature matching" method including improvements to avoid energy deviation induced by the non-linear effects previously observed [12, 16]. Then, the following beam tunings are done using the "with-reference method" (i.e. using a previous tuning as reference) allowing to tune a cavity phase without phase scan and without having to detune the downstream cavities, which allows a significant time saving. Finally, the third method, mainly used for heavy ion beams, allows to switch between ions at the same energy very quickly. In this case, the cavity phases were not modified while all the electric and magnetic fields of the accelerator were multiplied by the coefficient [17]

$$C = \frac{A_2/Q_2}{A_1/Q_1}$$

where A_1 and Q_1 are the mass and the charge of the reference ion and A_2 and Q_2 those of the new one.

The tuning used as reference in 2022 was a 5 mA H^+ beam at 33 MeV. From there, D^+ , $^4He^{2+}$ and $^{18}O^{6+}$ beams were tuned and accelerated using the "with-reference method" to 40 MeV and 7 MeV/A, respectively. Finally, starting from

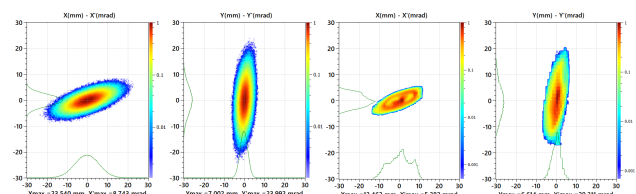
the tuning for the $^{18}O^{6+}$ and using the above-mentioned A/Q coefficient method, the $^{18}O^{7+}$ and $^{40}Ar^{14+}$ beams were transported in rebuncher mode (0.73 MeV/A) then accelerated to 7 MeV/A. Table 2 summarizes the parameters of the beams that have been tuned in SPIRAL2.

Table 2: Accelerated Heavy Ions in SPIRAL2

Parameter	$^{18}O^{6+}$	$^{18}O^{7+}$	$^{40}Ar^{14+}$
Max E (MeV/A)	7	7	7
Max I (μ A)	50	78	80
Transmission (%)	99	98	99
Beam power (kW)	1	0.6	1.6

Heavy Ion Results

The MEBT transverse emittances are in agreement with the expected ones for $^{18}O^{6+}$ beam as shown in Fig. 2. Transverse rms emittance measurements were 0.32 and 0.46 $\pi.mm.mrad$ in the horizontal and vertical planes, respectively. The Courant-Snyder parameters are in good agreement with the reference simulation in TraceWin (see Table 3) [18].

Figure 2: Transversal phase space in the MEBT for 0.7 mA $^{18}O^{6+}$ beam: reference simulation (left) and measurement (right).

The $^{18}O^{6+,7+}$ and $^{40}Ar^{14+}$ tunings were performed to obtain a final energy of 7 MeV/A, a value higher than that required for physics experiments at this time. To obtain this energy lower than the nominal energy (14 MeV/A), the cavities downstream cavity #15 were switched off and detuned, while the last cavity (#26) was used in rebuncher mode to reduce the energy spread. The $^{18}O^{6+}$ beam was accelerated to

Table 3: MEBT Simulated and Measured Courant-Snyder Parameters for 0.7 mA $^{18}\text{O}^{6+}$

Parameter	Sim	Meas	Δ (%)
$\alpha_{X,X'}$	-0.83	-0.99	19
$\beta_{X,X'}$ (mm/ π .mrad)	3.44	3.40	1
$\alpha_{Y,Y'}$	-0.29	-0.49	69
$\beta_{y,y'}$ (mm/ π .mrad)	0.32	0.38	19

7 MeV/A, $^{18}\text{O}^{7+}$ and $^{40}\text{Ar}^{14+}$ beams were then accelerated up to the same energy. The measured linac transmission was higher than 99% for $^{18}\text{O}^{6+}$ and for $^{18}\text{O}^{7+}$. To qualify the tuning quality, a power ramp up to 1 kW with a $^{18}\text{O}^{6+}$ beam at 7 MeV/A was performed. The strategy in this case was to accelerate the beam with a peak current of 50 μA through the linac and increase the pulse length up to 100% duty cycle. The evolution of the duty cycle and average current are shown in Fig. 3.

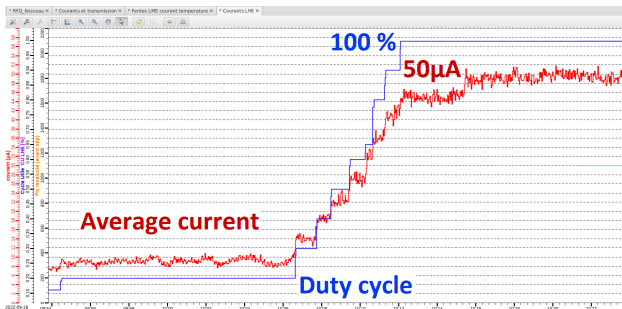


Figure 3: Power ramp up of 50 μA $^{18}\text{O}^{6+}$ beam: Duty cycle (blue) and average current (red).

The next step was to apply the A/Q method to switch to the $^{18}\text{O}^{7+}$ beam, and to optimise the beam transport in LBE1. After the particle switch without modifying any parameters in the linac, a 78 μA (peak current) $^{18}\text{O}^{7+}$ beam was accelerated up to 7 MeV/A as expected with a 1% duty cycle. The measured transmission was only 95% due to the fact that no transport optimisation was carried out after the switch. The same process was repeated to switch from $^{18}\text{O}^{6+}$ to $^{18}\text{O}^{7+}$ with an energy of 0.73 MeV/A, confirming the results obtained in the first study.

Finally, starting from the $^{18}\text{O}^{6+}$ tuning and applying the A/Q method, a 80 μA $^{40}\text{Ar}^{14+}$ beam was accelerated to 7 MeV/A. A power of 1.6 kW was achieved with a 100% duty cycle, and a maximum transmission higher than 99%. The Fig. 4 shows the evolution of the transmission and beam power during the power ramp up, the large variations in transmission were due to measurement electronics noise.

SPIRAL2 OPERATION

The beam time of SPIRAL2 in 2022 was approximately 3 months, starting on August 28 and ending on December 12. Seven physics experiments and three main preparatory studies for S^3 were conducted. Figure 5 shows the beam time distribution. The time for physics experiments repre-

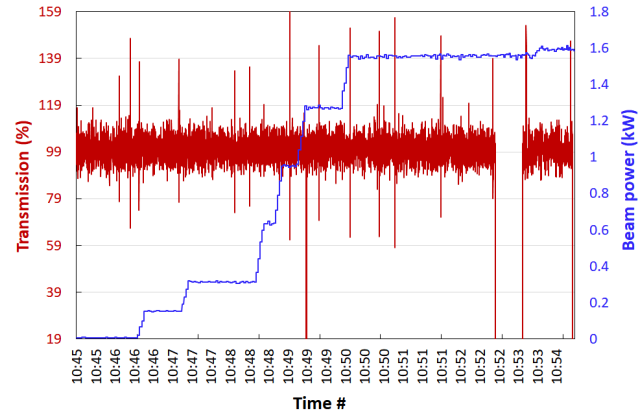


Figure 4: Power ramp up of 80 μA $^{40}\text{Ar}^{14+}$ beam: Transmission (red) and beam power (blue).

sented 49.8% of which 76% was with D^+ beams between 9 μA and 47 μA on the target, mainly with a selection of 1 bunch /100 using the SBS. The physics experiments were performed with H^+ , D^+ and $^{4}\text{He}^{2+}$ beams with energies from 10 MeV/A up to their nominal values. The tuning time comprises both accelerator and HEBT tunings. The latter includes HEBT switch from SAFARI to NFS with strict control and safety procedures. In 2022, accelerator trips were reduced from 32% to 8% compared to 2021.

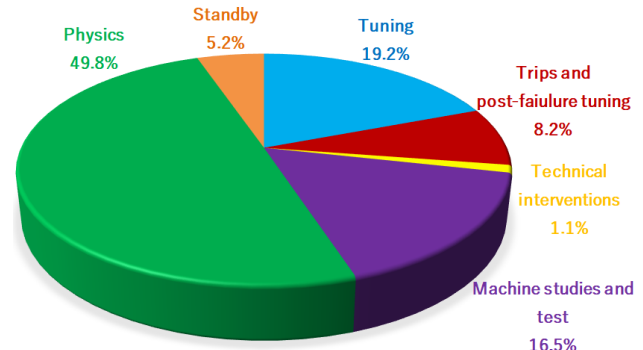


Figure 5: SPIRAL2 beam time sharing in 2022.

Concerning the 16.5% of the total time used for machine studies, 75% was used for beam dynamics studies with $^{4}\text{He}^{2+}$, D^+ , $^{18}\text{O}^{6+}$ and $^{40}\text{Ar}^{14+}$ beams. Tests were performed on: i) validation of the new reference and A/Q tuning methods as well as the implementation of the related EPICS applications [17], ii) the energy change procedure in full operation and iii) linac operation in case of cavity failure. For the energy change during an experiment, two methods were tested in order to study the losses and to be able to define a procedure, then to generate its application for an efficient operation. The final “energy change procedure” consists to define the last cavity to be used, where the output energy is the desired one, then all the downstream cavities must be detuned. The BRho coefficient is then applied to all the magnets up to the experimental room. Finally, a general alignment is done before delivering the beam again. The application is currently being developed to be used this year.

Preliminary results from the third study also showed that SPIRAL2 can deliver the beam in the event of cavity failure

in the high β section. In the case of low β cavity failure the beam transport without losses is impossible, then the tuning is very difficult at low energy due to a high debunching between two cavities. As the energy increases the debunching decreases, so if one of the last low β cavity fails, it is easier to recover a beam dynamics without losses. To do so, one must retune the downstream cavities to get the required phase acceptance, the price to pay being a reduction of the linac final energy and/or an obligation to increase the cavity voltages. Studies on this topic will continue this year.

The remaining “machine studies” time was spent mainly performing studies related to the RF and diagnostics systems.

This physics studies performed in the NFS room can be divided into three areas: i) neutron beam characterization, ii) production of quasi-monoenergetic or continuous spectrum neutron beams and iii) neutron beam induced reactions and activation. The NFS commissioning started the same year as the accelerator commissioning with successful measurements of proton-induced reaction cross sections and neutron beam characteristics. At the next stage, the results obtained in the production of effective ^{62}Zn or ^{54m}Co cross sections showed good agreement with previously published data as well as demonstrating the ability of the setup to study the production cross sections of short-lived isotopes. In 2022, the first experiment for neutron-induced reactions in a ^{235}U actinide target was carried out. The evolution of the energy and velocity distributions as a function of the incident neutron beam energy was detected with FALSTAFF [19, 20]. Preliminary results show that these measurements allow to determine the masses of the fragments successfully.

Accelerator Subsystems Issues and Improvements

The most relevant developments and aspects of cryogenic systems, beam diagnostics, MEBT beam dump enhancement, as well as the latest RF observations are discussed below.

Thermo-acoustic oscillations (TAO) were identified late in 2017 in each cold valves boxes of the LINAC. The pressure oscillation generated by the TAO was strong enough to prevent the use of the superconducting cavities. A temporary solution was developed and implemented. It restored the stability of the cryogenic system but had some drawbacks (periodical pressure perturbations, helium level sensors measuring range limitation). Therefore, a new TAO compensation system was developed: it is a RLC resonator which counterbalances the resonance. Resistance is provided by a micrometer needle valve, inductance by a length of tube, and capacitance by a helium storage volume. The new system was tested during the 2022 accelerator run and performed satisfactorily [21].

The development of a numerical model of the cryogenics system is an ongoing project which started in 2017 as a collaboration with CEA DSBT Grenoble. Using MatLab and the SimCryogenics library developed by DSBT, it was possible to build an accurate model of the cryomodules, which is the base of the linear quadratic (LQ) loop used for helium pressure and level control in the PLC. This same model was recently developed as a soft sensor. Based on the

helium parameters (level, pressure) and the control valves positions, the software is able to compute the heat load on the cryomodule helium bath. This feature, implemented in the cryogenics’ PLCs, has been tested during 2022. In particular, it helped to pinpoint a powerful field emission phenomenon in cavity #14 during the 2022 run, thus proving its usefulness. Developments are still ongoing in order to enhance the precision and the speed of the soft sensor.

A new electronics for the distribution of the RF reference signals to the BPM electronics was designed, manufactured and installed. The SPIRAL2 frequency at 88.0525 MHz is first distributed to the different RF systems: rebunchers, RFQ, cavities but also to the RF diagnostics such as BPM, Time-of-Flight (TOF) or BEM. The 2 RF reference signals (low β and high β sections) are distributed to the 20 electronic components of the BPM via distribution frames. The 3 distribution frames are adjusted to have a maximum phase difference of 0.5° between the outputs. These frames are also used to automate the electronics calibration. The calibration of a BPM module can be done remotely, by injecting 4 identical signals in amplitude and phase into the 4 inputs of a BPM electronics, thanks to two Calboxes that can be connected to the frames. Calibration of all BPMs was reduced from one week to three days, compared to previous calibrations.

Current measurements by the ACCT and DCCT located at the end of the MEBT had an offset of $\approx 100\text{ }\mu\text{A}$ in 2019. In the following run, it was found that the beam dump receiving the unused bunches deviated by the SBS ($\leq 7.5\text{ kW}$) was affected by Coulomb scattering producing an important heating degrading the beam current measurements. To reduce these effects, the beam dump was redesigned (surface changed from flat to staircase), constructed and installed, which successfully decreased the temperature and the current offset [22].

X-ray emissions have started from 2020 in cavities #2 (low β section) #14 and #26 (high β section). No modifications have been made to cavity #2 as its voltage is low and it is operating without problem under normal conditions. However, the voltage of cavities #14 and #26 had to be reduced (<8%) in order to run then reliability. To compensate, voltage of the neighbouring high β cavities has been increased; most of the high β cavities have been qualified and can operate up to 8 MV/m

FUTURE PERSPECTIVES

The SPIRAL2 beam time is planned to be progressively increased through parallel operation with the cyclotrons.

The S^3 experimental room is in its last phase of installation. Tests, measurements and conditioning works are currently being carried out on: target station, beam dump, electric dipole, superconducting multipole triplets, power-supply system and the associated cryogenic system [23]. The integration of the Super Separator Spectrometer - Low Energy Branch (S^3 -LEB) and laser system, the beam transport,

the start-up of physics, and the detection system commissioning are planned in 2024.

The low-energy beam experimental room “Decay, Excitation and Storage of Radioactive Ions” (DESIR) will be built in the next few years and will use ion beams from both GANIL/SPIRAL1 and SPIRAL2 facilities [24]. Nuclear physics, fundamental weak-interaction physics and astrophysics questions will be studied using laser spectroscopy techniques, decay spectroscopy of radioactive species, mass spectrometry and other trap-assisted measurements. The first civil engineering preparatory works have started at the beginning of this year and the building permit is currently in the process of public enquiry.

NEWGAIN is a new injector project which aims to produce and deliver ions with mass to charge ratio $A/Q \leq 7$ to the linac. The design phase started on May 2020. The preliminary design study phase was completed in June 2021 and the project is currently in the detailed design study phase [25]. The injector will be located in an existing cave in the SPIRAL2 building as shown in Fig. 6.



Figure 6: SPIRAL2 NEWGAIN injector.

CONCLUSIONS

The SPIRAL2 SC linac has been running successfully in 2022, during its first year of nominal operation. Half beam time has been used for NFS physics experiments, the remaining time being used for beam dynamics checks, RF and diagnostics system improvements. For the preparatory phase of S^3 , $^{18}O^{6+,7+}$ and $^{40}Ar^{14+}$ beams ($\leq 80\mu A$) were accelerated for the first time in the linac up to 7 MeV/A.

REFERENCES

- [1] A.K. Orduz *et al.*, “Commissioning of a high power linac at GANIL: Beam power ramp-up,” *Phys. Rev. Accel. Beams*, vol. 25, pp. 060101, 2022. doi:10.1103/PhysRevAccelBeams.25.060101
- [2] H. Goutte and N. Alahari, “Microscopes for the Physics at the Femtoscale: GANIL-SPIRAL2,” *Nuclear Physics News*, vol. 31, pp. 5–12, 2021. doi:10.1080/10619127.2021.1881363.
- [3] O. Kamalou *et al.*, “Status Report on GANIL and Upgrade of SPIRAL1” in *Proc. 22nd. Int. Conf. on Cyclotrons and their Applications (CYC2019)*, Cape Town, South Africa, Sep. 2019, pp. 09-11. doi:10.18429/JACoW-Cyclotrons2019-MOA03
- [4] J-L. Biarrotte and P. Bertrand and D. Uriot, “Beam Dynamics Studies for the SPIRAL2 Project” in *European Particle Accelerator Conf. (EPAC'06)*, Edinburgh, United Kingdom, Jun. 2006, pp. 1930-1932. doi:10.18429/JACoW-HIAT2015-MOA1C02.
- [5] R. Ferdinand *et al.*, “Final Results of the SPIRAL2 Injector Commissioning,” in *Proc. 10th Int. Particle Accelerator Conf. (IPAC'19)*, Melbourne, Australia, May. 2019, pp. 848-851. doi:10.18429/JACoW-IPAC2019-TUPT5007.
- [6] M. Di Giacomo *et al.*, “Proton beam commissioning of the SPIRAL2 Single Bunch Selectors,” *Journal of Instrumentation*, vol. 15, p. T12011, 2020. doi:10.1088/1748-0221/15/12/T12011.
- [7] G. Orly *et al.*, “Spiral2 cryomodules B tests results,” in *Proc. 16th Int. Conf. on RF Superconductivity (SFR2013)*, Paris, France, Sep. 2013, paper MOP010, .pp. 95-99.
- [8] C. Marchand *et al.*, “Performances of Spiral2 Low and High Beta Cryomodules,” in *Proc. 17th Int. Conf. on RF Superconductivity (SFR2015)*, MWhistler, Canada, Dec. 2015, pp. 967-972. doi:10.18429/JACoW-SRF2015-WEBA04.
- [9] X. Ledoux *et al.*, “The neutrons for science facility at SPIRAL2” *EPJ Web Conf.*, vol. 146, pp. 03003, 2017. doi:10.1051/epjconf/201714603003
- [10] A. Drouart *et al.*, “The Super Separator Spectrometer (S^3) for SPIRAL2 stable beams” *Nuclear Physics A*, vol. 834, pp. 747c-750c, 2010. doi:10.1016/j.nuclphysa.2010.01.135
- [11] C. Jamet *et al.*, “SPIRAL2 Diagnostic Qualifications with RFQ beams,” in *Proc. 8th Int. Beam Instrumentation Conf. (IBIC'19)*, Malmo, Sweden, Sep. 2019, pp. 188-192. doi:10.18429/JACoW-IBIC2019-MOPP036.
- [12] A.K. Orduz *et al.*, “SPIRAL2 Final Commissioning Results,” in *Proc. 31st Int. Linear Accelerator Conf. (IPAC'22)*, Liverpool, UK, Aug. 2022, pp. 314-318. doi:10.18429/JACoW-LINAC2022-TU2AA02.
- [13] X. Ledoux *et al.*, “First beams at neutrons for science” *Eur. Phys. J. A*, vol. 57, pp. 257, 2021. doi:10.1140/epja/s10050-021-00565-x
- [14] A.K. Orduz *et al.*, “Deuteron Beam Power Ramp-Up at SPIRAL2,” in *Proc. 13th Int. Particle Accelerator Conf. (IPAC'22)*, Bangkok, Thailand, Jun. 2022, pp. 70-73. doi:10.18429/JACoW-IPAC2022-MOPST010.
- [15] E. Schibler and L. Perrot, “SAFARI, an Optimized Beam Stop Device for High Intensity Beams at the Spiral2 Facility,” in *Proc. 2nd Int. Particle Accelerator Conf. (IPAC2011)*, San Sebastian, Spain, Sep. 2022, pp. 1162-1164.
- [16] T.L. Owens *et al.*, “Phase scan signature matching for linac tuning,” in *Proc. 17th Int. Linac Conf. (LINAC94)*, Tsukuba, Japan, Aug. 1994, pp. 169–179.
- [17] G. Normand *et al.*, “Strategies For SPIRAL2 Linac Heavy-Ion Beam Tuning,” presented at the 14th Int. Particle Accelerator Conf. Conf. IPAC'23), Venice, Italy, May 2023, paper TUPA192, this conference.
- [18] D. Uriot and N. Pichoff, “Status of TraceWin Code,” in *Proc. 6th Int. Particle Accelerator Conf. (IPAC2015)*, Richmond, VA, United States, May. 2015, pp. 92-94. doi:10.18429/JACoW-IPAC2015-MOPWA008.

[19] S. Panebianco *et al.*, "FALSTAFF/ a novel apparatus for fission fragment characterization" *EPJ Web Conf.*, vol. 69, pp. 00021, 2014. doi:10.1051/epjconf/20146900021

[20] First experience with FALSTAFF at NFS, GANIL, <https://www.ganil-spiral2.eu/2023/02/27/first-experience-with-falstaff-at-nfs/>

[21] A. Ghrib *et al.*, "Cryogenic thermoacoustics in the SPIRAL2 LINAC," *Cryogenics*, vol. 124, pp. 103487, 2022. doi.org/10.1016/j.cryogenics.2022.103487

[22] M. Di Giacomo *et al.*, "Upgrade of the medium energy beam dump geometry for the SPIRAL2 single bunch selector," presented at the 14th Int. Particle Accelerator Conf. Conf. IPAC'23, Venice, Italy, May 2023, paper THPA190, this conference.

[23] A. Esper *et al.*, "Superconducting Multipole Triplet Field Measurements," presented at the 14th Int. Particle Accelerator Conf. Conf. IPAC'23, Venice, Italy, May 2023, paper THPA043, this conference.

[24] DESIR, GANIL, <https://heberge.lp2ib.in2p3.fr/desir/-Description-of-the-DESIR-facility->

[25] M.H. Moscatello *et al.*, "NEWGAIN project at GANIL-SPIRAL2 : design of the new heavy ion injector for the superconducting LINAC," presented at the 14th Int. Particle Accelerator Conf. Conf. IPAC'23, Venice, Italy, May 2023, paper TUPA193, this conference.